

From 7T to 10.5T: B₁⁺, SAR and Temperature Distribution for Head and Body MRI

Jinfeng Tian¹, Devashish Shrivastava¹, John Strupp¹, Jay Zhang¹, and Thomas Vaughan¹
¹U. of Minnesota, Minneapolis, MN, United States

INTRODUCTION

Since the installation of the first 7T whole-body MRI system in 1999, numerous researches have been carried on the 7T human machines. Spurred by the high-field advantages and success, over 30 whole-body MRI systems have been installed world wide and more are expected in following years. To push the boundary of high field MRI research further forward, a whole-body MRI at 10.5T will be installed early next year. History reveals that the high field benefits can be realized at the system only after technical challenges, especially the RF changes, are met [1-3]. The study intends to provide a peek into the RF performance variation from 7T to 10.5T, which correspond to the Larmor frequencies of 300MHz (7T) and 450MHz (10.5T) for proton nuclear.

METHOD and MATERIALS

A 16-channel TEM body coil array with co-axial elements was simulated with Sencad (Speag, Switzerland): length=200mm, coil diameter=572mm, RF shielding inner diameter=630mm. A 33-year-old adult male, Duke (180cm, 72kg), from Virtual Family, was loaded in the array in two ways: the head and the heart at coil center (Fig. 1). The coil was tuned to 300MHz and 450MHz with the loading. The 16-channel was driven in quadrature mode, with a total RF input RF power of 16W for head and 144W for body simulation. The SAR from the EM simulation was then employed as one thermal source in following thermal calculation with Pennes' equation.

Results

The results are illustrated in Figure 2 and 3, together with the mean $|B_1^+|$ in three central slices and the global maximum 1gram and 10gram SAR in Table 1.

For the simulation setup described, following results can be observed: 1) from 7T to 10.5T, the RF field and energy in body MRI tends to increase in the head and decrease in the lower half of the body, though the heart is located at coil center. The transmission efficiency ($|B_1^+|/\sqrt{\text{Watt}}$) is low and comparable at both frequencies within the 16cmx16cmx20cm FOV. 2) The transmission efficiency of head MRI drops quickly from 7T to 10.5T. 3) To get same $|B_1^+|$, the maximum local SARs are much higher (>50%) at 10.5T than those at 7T. For body MRI, both the maximum 1gram and 10gram SARs occur at the arm, which is close to the coil. If arms are excluded, the maximum local SARs, located at the neck or cerebellum at both frequencies, are much lower. 4) The RF artifacts, including two black lines with weak $|B_1^+|$ in body MRI and the center brightness in head MRI, are similar for two frequencies but more severe at 10.5T. 4). The temperature rise is larger at 10.5T, with maximum rises at the upper arms, neck, and tissues in lower half of the head.

Discussions and Conclusions

1). The TEM array provides a peak of the RF performance and human body's response to EM waves at 7T and 10.5T. But the array is large and far from the body, thus creating difficulties in managing RF power distribution within human body. Other measures could improve the situation: thin dielectric layers in guiding the RF energy flowing, and/or small-sized arrays placed close to the image region of interest, together with the aid of static and dynamic RF shimming techniques; 2) special attention is required for the RF safety during MRI at 10.5T due to the higher SAR and temperature; 3) the increased RF gradient may indicate suggest smaller RF shimming region at 10.5T than at 7T; 4). Temperatures simulated using Pennes' equation may underestimate the heating problem due to Pennes blood sink approximation.

References

[1] Vaughan JT, MRM 32:206-218. [2]. Adriany G, MRM 53: 434-435. [3]. Metzger G, MRM 59: 396-409.

Acknowledgment: NIH-NIBIB-EB000895, NIH-NIBIB-EB006835, NIH-NIBIB-EB007327, NIH-NCRR-P41-RR08079, P41 - RR008079

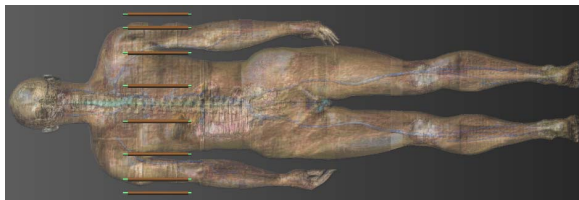


Figure 1. The TEM array and the Duke body model with heart located at coil center. The RF shielding was removed to better demonstrate the structures. For head MRI simulation, the brain was at coil iso-center.

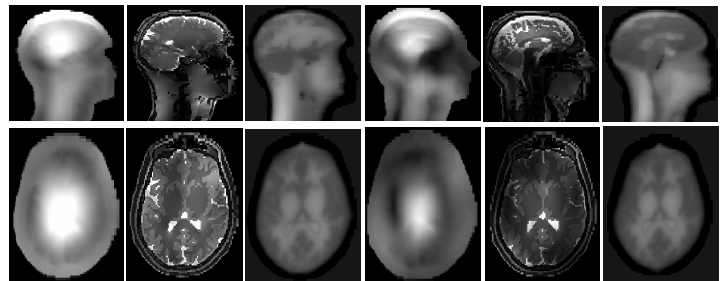


Figure 3. The $|B_1^+|$, SAR and Temperature (T) distribution for head MRI. The illustrations are in the same order as given in Figure 2, but with different linear ranges. $|B_1^+|$: [0 1.2] μ T. SAR: [0. 4.8] W/kg. and Temperature: [36.9. 38]°C.

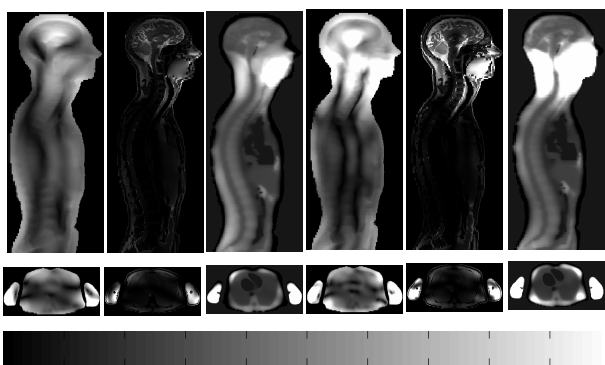


Figure 2. The $|B_1^+|$, SAR and Temperature distribution for body MRI in (top row) the central sagittal slices and (middle row) the central transverse slices. For the first two rows, the illustrations are (from left to right) in the order of: $|B_1^+|$, SAR and Temperature at 7T, and $|B_1^+|$, SAR and T at 10.5T. The gray color-bar is given in the bottom row. All illustrations are in linear scales with following ranges, $|B_1^+|$: [0 1.2] μ T, SAR: [0, 14.4] W/kg, and Temperature: [36.9, 38]°C.

Table 1. The mean $|B_1^+|$ on the central slices, and the maximum local SAR averaged over 1g and 10g tissues. In averaging $|B_1^+|$ for the body MRI, a FOV of 16cmx16cmx20cm was used, which excluded the arms and had the same length as the TEM array. For head MRI, the average was done within the whole head. The SAR data in the '()' for body MRI is the maximum SAR in the torso, without SAR in the arms are counted. *1: the max SAR occurs within muscle in the left arm, *2: cerebellum in the lower brain, *3: within the muscle in the neck, *4: CSF in the top brain.

	$ B_1^+ $ Magnitude averaged on central slices (μ T)			Max. local SAR (W/kg) Averaged within	
	Transverse	Sagittal	Coronal	1g	10g
7T, Body	0.564	0.600	0.480	40.32 ^{*1} (11.52 ^{*2})	35.52 ^{*1} (7.69 ^{*3})
10.5T, Body	0.384	0.708	0.564	72.26 ^{*1} (19.71 ^{*3})	54.43 ^{*1} (16.65 ^{*3})
7T, Head	1.616	1.812	1.856	6.880 ^{*4}	4.336 ^{*4}
10.5T, Head	0.604	0.792	0.816	5.056 ^{*4}	3.920 ^{*4}